

Boundary integral multi-trace formulations and Optimised Schwarz Methods

Xavier Claeys, Pierre Marchand

▶ **To cite this version:**

Xavier Claeys, Pierre Marchand. Boundary integral multi-trace formulations and Optimised Schwarz Methods. Computers & Mathematics with Applications, 2020, 79 (11), 10.1016/j.camwa.2020.01.016 . hal-01921113

HAL Id: hal-01921113
https://inria.hal.science/hal-01921113

Submitted on 13 Nov 2018

HAL is a multi-disciplinary open access archive for the deposit and dissemination of scientific research documents, whether they are published or not. The documents may come from teaching and research institutions in France or abroad, or from public or private research centers.

L'archive ouverte pluridisciplinaire **HAL**, est destinée au dépôt et à la diffusion de documents scientifiques de niveau recherche, publiés ou non, émanant des établissements d'enseignement et de recherche français ou étrangers, des laboratoires publics ou privés.

Boundary integral multi-trace formulations and Optimised Schwarz Methods

X.Claeys*, P.Marchand*

Abstract

In the present contribution, we consider Helmholtz equation with material coefficients being constants in each subdomain of a geometric partition of the propagation medium (discarding the presence of junctions), and we are interested in the numerical solution of such a problem by means of local multi-trace boundary integral formulations (local-MTF). For a one dimensional problem and configurations with two subdomains, it has been recently established that applying a Jacobi iterative solver to local-MTF is exactly equivalent to an Optimised Schwarz Method (OSM) with a non-local impendance. In the present contribution, we show that this correspondance still holds in the case where the subdomain partition involves an arbitrary number of subdomains. From this, we deduce that the depth of the adjacency graph of the subdomain partition plays a critical role in the convergence of linear solvers applied to local-MTF: we prove it for the case of homogeneous propagation medium and show, through numerical evidences, that this conclusion still holds for heterogeneous media. Our study also shows that, considering variants of local-MTF involving a relaxation parameter, there is a fixed value of this relaxation parameter that systematically leads to optimal speed of convergence for linear solvers.

Keywords— Domain Decomposition, Optimized Schwarz Method, boundary integral formulation, multi-domain, Helmholtz

Introduction

To deal with the the numerical simulation of harmonic wave propagation in piecewise constant media, multi-trace formulations (MTF) have been introduced some years ago as a new family of boundary integral equations. As a salient feature, these formulations rely on doubling unknown traces at each point of each interface, and the traces on the boundary of a subdomain are a priori disconnected from the traces on the boundary of other subdomains. This apparent decoupling of the traces renders MTF a natural framework for rolling out a domain decomposition (DDM) methodology. Transmission conditions are enforced only weakly, by means of a transmission operator.

There exist several variants of MTF that differ through the corresponding choice of transmission operators. From a DDM perspective, the most appealing variant appears to be the so-called local-MTF [9] because, in this case, the transmission operator acts by exchanging

*Sorbonne Université, Université Paris-Diderot SPC, CNRS, Inria, Laboratoire Jacques-Louis Lions, équipe Alpines, F-75005 Paris

the traces of neighbouring subdomains and it is thus local. After discretization of this transmission operator, the corresponding matrix is block sparse, each block being a surface mass matrix supported on a single interface.

In the context of domain decomposition, the analysis of block linear solvers applied to multi-trace formulations arises as a natural question. In [10] the authors introduced new variants of local-MTF involving a relaxation parameter α that could be used to improve the performance of linear solvers. With the convention of the present contribution, the original local-MTF corresponds to the value $\alpha = 0$. Very few analysis was proposed in [10] regarding a proper tuning of this parameter. A first detailed discussion on this point was proposed in [7], where an elementary situation in 1D with two subdomains and one interface was studied. Considering a Jacobi linear solver, the discussion in [7] pointed to a critical value of the relaxation parameter $\alpha = 1$ that minimizes the spectral radius of the Jacobi iteration. This discussion was extended to two and three subdomains in arbitrary dimensions in [3], for a strongly elliptic equation. Considering a one dimensional problem paritionned in two subdomains, the authors in [3] observed that the local-MTF with relaxation parameter $\alpha = 1$ can be identified as a particular instance of the Optimised Schwarz Method (OSM) in a configuration with two subdomains and one interface involving no material contrast in the coefficients of the PDE. The first goal of the present contribution is to show that this identification between OSM and local-MTF still holds for more general configurations with arbitrary number of subdomains (rulling out the presence of junction points though).

The fastest convergence of Jacobi solvers is reached for $\alpha = 1$: this was clearly put into evidence in [3, 7] for the case of positive strongly elliptic problems. However for Helmholtz equation, in most cases, Jacobi solvers do not converge anymore. Yet, considering a Krylov type solver, one may ask what is the value of α leading to the fastest convergence. In the present contribution, on the basis of numerical results, we show that $\alpha = 1$ remains the optimal value with GMRes as linear solver.

The analysis presented in [3, 7] does not hold anymore with constrasts in material caracteristics and varying coefficients of the PDE. This was partly adressed in [2] that proposed a detailed study of the essential spectrum of the local-MTF operator for Helmholtz equation $\Delta u + \kappa^2 u = 0$ with piecewise constant wave number κ. However [2] did not discuss the convergence of linear solvers. In the present contribution, we show how the results of [2] lead to nilpotence of the Jacobi iteration operator for the case of constant material caracteristics. Finally considering an equation of the form $\mathrm{div}(\mu^{-1}\nabla u) + \kappa^2 u = 0$ with contrasts in both μ and κ, we present numerical results suggesting that the conclusions [3, 7] remain valid.

The outline of this article is as follows. In the first section we describe in detail the geometrical configurations and the scalar wave scattering problem that we wish to consider i.e. Helmholtz equation with piecewise constant coefficients, with contrasts appearing both in the wave number and in the principal part of the operator. In the second section we fix notations related to function spaces and trace operators, and in the third section we review classical results related to boundary integral equations. The fourth section is dedicated to a detailed analysis of Calderón projectors in a multi-domain context. In section 5 we derive the local multi-trace formulation and, in Section 6 we discuss the block-Jacobi iterative scheme applied to this formulation and we show that, for homogeneous propagation media, the Jacobi method converges in a number of steps connected to the depth of the adjacency graph of the subdomain partition. In Section 7 we show that local-MTF can be considered as a particular instance of Optimized Schwarz Method (OSM). The last section is dedicated to the presentation of various numerical results, considering two geometrical configurations (one with stable depth

of the adjacency graph, and one with growing depth) and paying attention to cases with varying material caracteristics.

1 Problem under consideration

Let us describe the problem under consideration for the remaining of this contribution. Let $d = 2$ or 3 refer to the dimension of the ambient space. We shall consider a non-overlapping partition of the space $\mathbb{R}^d = \cup_{j=0}^{n} \overline{\Omega}_j$, where the Ω_j's are Lipschitz open sets with $\Omega_j \cap \Omega_k = \emptyset$ for $j \neq k$, and all Ω_j are bounded except Ω_0. The boundaries will be denoted $\Gamma_j := \partial\Omega_j$, and $\Gamma_{j,k} := \Gamma_j \cap \Gamma_k$. We will also make the strong assumption that the geometrical configuration does not involve any junction point, which can be rewritten

$$\begin{array}{l} \Gamma_j \cap \Gamma_k \cap \Gamma_l = \emptyset \\ \text{for } j \neq k,\ k \neq l,\ l \neq j \end{array} \tag{1}$$

We consider an equation modeling propagation of acoustic waves in harmonic regime. Let $\varpi > 0$ refer to the pulsation of the wave. We consider two positive functions $\mu, \varrho : \mathbb{R}^d \to (0, +\infty)$ supposed to be constant in each subdomain, and denote $\mu_j = \mu|_{\Omega_j} > 0$ and $\varrho_j = \varrho|_{\Omega_j} > 0$. Then we consider the problem

$$\begin{cases} \operatorname{div}(\mu^{-1}(\boldsymbol{x})\nabla u) + \varpi^2 \varrho(\boldsymbol{x}) u = 0 \quad \text{in } \mathbb{R}^d, \\ u - u_{\text{inc}} \ \ \kappa_0\text{-outgoing radiating.} \end{cases} \tag{2}$$

In this problem $u_{\text{inc}} \in \mathrm{L}^2_{\text{loc}}(\mathbb{R}^d)$ refers to any function satisfying the wave equation of the exterior domain $\mu_0^{-1}\Delta u_{\text{inc}} + \varpi^2 \varrho_0 u_{\text{inc}} = 0$ in $\mathbb{R}^d$. Plane waves $u_{\text{inc}}(\boldsymbol{x}) = \exp(\imath\kappa_0 \boldsymbol{\nu}\cdot\boldsymbol{x})$ for fixed $\boldsymbol{\nu} \in \mathbb{R}^d, |\boldsymbol{\nu}| = 1$ and $\kappa_0 := \varpi\sqrt{\mu_0\varrho_0}$ fit this assumption. The outgoing radiation condition, also known as Sommerfeld's radiation condition, writes

$$v\ \kappa_0\text{-outgoing radiating} \quad \Longleftrightarrow \quad \lim_{r\to\infty} \int_{\partial \mathrm{B}_r} |\partial_r v - \imath\kappa_0 v|^2 d\sigma_r = 0 \tag{3}$$

where B_r is the ball of radius r centered at 0, and σ_r refers to its surface measure. For more details about Sommerfeld's radiation condition, we refer the reader to e.g. [13, §2.6]. For the sequel, let $\kappa_j := \varpi\sqrt{\mu_j\varrho_j}$ refer to the effective wave number in subdomain Ω_j. Problem (2) can be rewritten equivalently as a system of $n+1$ wave equations coupled through interfaces by transmission conditions,

$$\begin{cases} \Delta u + \kappa_j^2 u = 0 \quad \text{in } \Omega_j \\ u - u_{\text{inc}} \ \ \kappa_0\text{-outgoing radiating} \end{cases} \tag{4}$$

$$\begin{cases} \mu_j^{-1}\partial_{\boldsymbol{n}_j} u|_{\Gamma_j} + \mu_k^{-1}\partial_{\boldsymbol{n}_k} u|_{\Gamma_k} = 0 \\ u|_{\Gamma_j} - u|_{\Gamma_k} = 0 \qquad \text{on } \Gamma_j \cap \Gamma_k \end{cases} \tag{5}$$

In the transmission conditions (5), the traces at Γ_j should be understood as taken from the interior of Ω_j, and $\partial_{\boldsymbol{n}_j}$ refers to the normal derivative at Γ_j with normal vector field $\boldsymbol{n}_j$ directed toward the exterior of Ω_j.

2 Function spaces

In the sequel, for $\Omega \subset \mathbb{R}^d$ a Lipschitz open set, denote $\Gamma := \partial\Omega$ its boundary. The space $\mathrm{L}^2(\Omega)$ will, as usual, refer to the space of square integrable measurable functions equipped with the norm $\|v\|^2_{\mathrm{L}^2(\Omega)} := \int_\Omega |v| d\boldsymbol{x}$, and $\mathrm{H}^1(\Omega) := \{v \in \mathrm{L}^2(\Omega),\ \nabla v \in \mathrm{L}^2(\Omega)\}$ equipped with the norm $\|v\|^2_{\mathrm{H}^1(\Omega)} := \|v\|^2_{\mathrm{L}^2(\Omega)} + \|\nabla v\|^2_{\mathrm{L}^2(\Omega)}$. It is well established that the so-called Dirichlet trace operator

$$\gamma^\Omega_{\mathrm{D}}(\varphi) := \varphi|_{\partial\Omega}, \qquad \varphi \in \mathscr{C}^\infty(\overline{\Omega}) \tag{6}$$

can be extended as a continuous map $\gamma^\Omega_{\mathrm{D}} : \mathrm{H}^1(\Omega) \to \mathrm{L}^2(\partial\Omega)$, and its range $\mathrm{H}^{1/2}(\partial\Omega) := \mathrm{range}(\gamma^\Omega_{\mathrm{D}})$ turns out to be an Hilbert space when equipped with the following choice of norm $\|v\|_{\mathrm{H}^{1/2}(\partial\Omega)} = \min\{\|u\|_{\mathrm{H}^1(\Omega)},\ \gamma^\Omega_{\mathrm{D}}(u) = v\}$. Its topological dual space $\mathrm{H}^{-1/2}(\partial\Omega) = \mathrm{H}^{1/2}(\partial\Omega)'$ will be equipped with the associated dual norm

$$\|p\|_{\mathrm{H}^{-1/2}(\partial\Omega)} := \sup_{v \in \mathrm{H}^{1/2}(\partial\Omega)\setminus\{0\}} \frac{|\langle p, v\rangle_{\partial\Omega}|}{\|v\|_{\mathrm{H}^{1/2}(\partial\Omega)}} \tag{7}$$

where we have denoted $\langle\cdot,\cdot\rangle_{\partial\Omega}$ the duality pairing between $\mathrm{H}^{1/2}(\partial\Omega)$ and $\mathrm{H}^{-1/2}(\partial\Omega)$. Defining $\mathrm{H}^1(\Delta,\Omega) := \{v \in \mathrm{H}^1(\Omega),\ \Delta v \in \mathrm{L}^2(\Omega)\}$ equipped with the norm $\|v\|^2_{\mathrm{H}^1(\Delta,\Omega)} := \|v\|^2_{\mathrm{H}^1(\Omega)} + \|\Delta v\|^2_{\mathrm{L}^2(\Omega)}$, the so-called Neumann trace operator

$$\gamma^\Omega_{\mathrm{N}}(\varphi) := \boldsymbol{n}_\Omega \cdot \nabla\varphi|_{\partial\Omega} \qquad \varphi \in \mathscr{C}^\infty(\overline{\Omega}), \tag{8}$$

can be extended as a continuous map from $\mathrm{H}^1(\Delta,\Omega)$ onto $\mathrm{H}^{-1/2}(\partial\Omega)$, where $\boldsymbol{n}_\Omega$ refers to the normal vector at Γ directed toward the exterior of Ω. We also need to introduce $\gamma^\Omega : \mathrm{H}^1(\Delta,\Omega) \to \mathrm{H}^{1/2}(\partial\Omega) \times \mathrm{H}^{-1/2}(\partial\Omega)$ defined by

$$\gamma^\Omega(\varphi) := (\gamma^\Omega_{\mathrm{D}}(\varphi), \gamma^\Omega_{\mathrm{N}}(\varphi)). \tag{9}$$

This trace operator maps into the space of pairs of Dirichlet/Neumann traces $\mathcal{H}(\Gamma) := \mathrm{H}^{1/2}(\Gamma)\times\mathrm{H}^{-1/2}(\Gamma)$ equipped with the natural cartesian product norm $\|(v,q)\|^2_{\mathcal{H}(\Gamma)} := \|v\|^2_{\mathrm{H}^{1/2}(\Gamma)} + \|q\|^2_{\mathrm{H}^{-1/2}(\Gamma)}$. This space is realised as its own topological dual through the bilinear pairing $[\cdot,\cdot]_\Gamma : \mathcal{H}(\Gamma) \times \mathcal{H}(\Gamma) \to \mathbb{C}$ defined by

$$\begin{aligned} &[(u,p),(v,q)]_\Gamma := \langle u, q\rangle_\Gamma - \langle v, p\rangle_\Gamma \\ &\forall u, v \in \mathrm{H}^{+\frac{1}{2}}(\Gamma),\ \forall p, q \in \mathrm{H}^{-\frac{1}{2}}(\Gamma). \end{aligned} \tag{10}$$

We also introduce γ^Ω_c, $\gamma^\Omega_{\mathrm{D},c}$, $\gamma^\Omega_{\mathrm{N},c}$ defined in the same manner as γ^Ω, $\gamma^\Omega_{\mathrm{D}}$, $\gamma^\Omega_{\mathrm{N}}$ with traces taken from the exterior. In particular, in the definition of $\gamma^\Omega_{\mathrm{N},c}$, the normal vector is still assumed to be directed toward the exterior of Ω. The jump and average traces are defined by

$$\begin{aligned} &[\gamma^\Omega] := \gamma^\Omega - \gamma^\Omega_c, \\ &\{\gamma^\Omega\} := (\gamma^\Omega + \gamma^\Omega_c)/2. \end{aligned} \tag{11}$$

Denote for a moment $\Omega_c = \mathbb{R}^d\setminus\overline{\Omega}$ and let $\boldsymbol{n}_c$ refer to the normal vector field to $\Gamma = \partial\Omega$ pointing toward the exterior of Ω_c (hence pointing toward the interior of Ω). Let us emphasize that γ^Ω_c

does not coincide with γ^{Ω_c}. These trace operators are both taken from the interior of Ω_c but they are different due to $\boldsymbol{n} = -\boldsymbol{n}_c$. To be more explicit we have

$$\gamma^{\Omega_c} = \mathrm{Q} \cdot \gamma_c^{\Omega} \quad \text{where} \quad \mathrm{Q} := \begin{bmatrix} 1 & 0 \\ 0 & -1 \end{bmatrix}. \tag{12}$$

From this we also deduce that $\{\gamma^{\Omega_c}\} = \mathrm{Q} \cdot \{\gamma_c^{\Omega}\}$ and $[\gamma^{\Omega_c}] = -\mathrm{Q} \cdot [\gamma^{\Omega}]$. These elementary identities will prove handy later on.

3 Potential theory

Now we introduce classical potential and integral operators associated with homogeneous Helmholtz equation in each subdomain. Through this paragraph Ω will refer to a Lipschitz open set that is either bounded or the complementary to a bounded domain. For a given $\kappa > 0$, denote $\mathscr{G}_\kappa(\boldsymbol{x}) := \exp(\imath\kappa|\boldsymbol{x}|)/(4\pi|\boldsymbol{x}|)$ the outgoing Green kernel for Helmholtz equation. Next, for $\mathfrak{u} = (u, p) \in \mathcal{H}(\Gamma) := \mathrm{H}^{1/2}(\Gamma) \times \mathrm{H}^{-1/2}(\Gamma)$, we consider the potential operator

$$\begin{aligned} \mathrm{G}_\kappa^{\Omega}(\mathfrak{u})(\boldsymbol{x}) := & \int_\Gamma \boldsymbol{n}(\boldsymbol{y}) \cdot (\nabla \mathscr{G}_\kappa)(\boldsymbol{x} - \boldsymbol{y}) u(\boldsymbol{y}) d\sigma(\boldsymbol{y}) \\ & + \int_\Gamma \mathscr{G}_\kappa(\boldsymbol{x} - \boldsymbol{y}) p(\boldsymbol{y}) d\sigma(\boldsymbol{y}). \end{aligned} \tag{13}$$

The first term in the right hand side above is known as double layer potential, and the second term is known as single layer potential. The potential $\mathrm{G}_\kappa^{\Omega}$ induces a continuous map from $\mathcal{H}(\Gamma)$ into $\mathrm{H}^1_{\mathrm{loc}}(\Delta, \overline{\Omega}) \times \mathrm{H}^1_{\mathrm{loc}}(\Delta, \mathbb{R}^d \setminus \Omega)$, see e.g [14, Thm.3.1.16]. For $\Omega_c = \mathbb{R}^d \setminus \overline{\Omega}$, observe that we have $\mathrm{G}_\kappa^{\Omega} \cdot \mathrm{Q} = -\mathrm{G}_\kappa^{\Omega_c}$. When combined with trace operators, it yields a representation of any solution to the homogeneous Helmholtz equation inside Ω, see e.g [14, Thm.3.1.8].

Proposition 3.1.
Let $u \in \mathrm{H}^1_{\mathrm{loc}}(\Delta, \overline{\Omega})$ refer to any solution to the homogeneous Helmholtz equation $\Delta u + \kappa^2 u = 0$ in Ω. Assume in addition that u is κ-outgoing radiating if $\mathbb{R}^d \setminus \Omega$ is bounded. Then we have

$$\mathrm{G}_\kappa^{\Omega}(\gamma^{\Omega}(u))(\boldsymbol{x}) = u(\boldsymbol{x}) 1_\Omega(\boldsymbol{x}) \quad \forall \boldsymbol{x} \in \mathbb{R}^d.$$

Similarly if $v \in \mathrm{H}^1_{\mathrm{loc}}(\Delta, \overline{\Omega})$ satisfies $\Delta v + \kappa^2 v = 0$ in $\mathbb{R}^d \setminus \overline{\Omega}$ (and v is κ-outgoing if Ω is bounded), then $\mathrm{G}_\kappa^{\Omega}(\gamma_c^{\Omega}(v))(\boldsymbol{x}) = -v(\boldsymbol{x}) 1_{\mathbb{R}^d \setminus \Omega}(\boldsymbol{x})$ for all $\boldsymbol{x} \in \mathbb{R}^d$.

In the proposition 1_Ω (resp. $1_{\mathbb{R}^d \setminus \Omega}$) refers to the characteristic function of the set Ω (resp. $\mathbb{R}^d \setminus \Omega$). The potential operator satisfies the so-called jump formulas that can be summarised by the identity

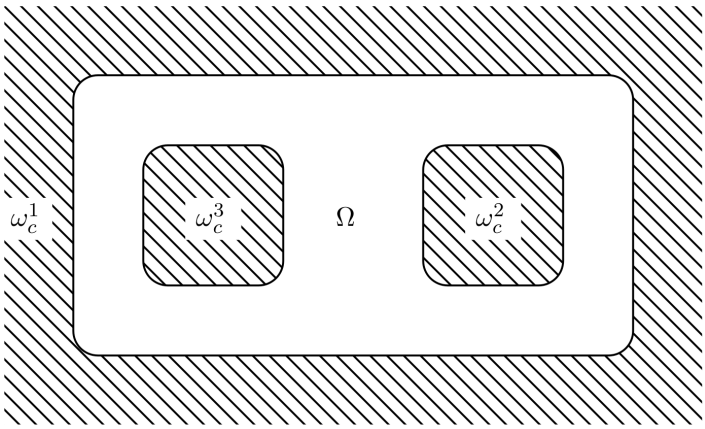
$$[\gamma^{\Omega}] \cdot \mathrm{G}_\kappa^{\Omega} = \mathrm{Id}. \tag{14}$$

Both terms in the identity above should be understood as continuous operators mapping $\mathcal{H}(\Gamma)$ into $\mathcal{H}(\Gamma)$. The representation theorem above involves a particular class of traces obtained from solutions to the homogeneous Helmholtz equation. This leads to the introduction of the space

$$\mathcal{C}_\kappa^+(\Omega) := \{\gamma(u),\ u \in \mathrm{H}^1_{\mathrm{loc}}(\Delta, \overline{\Omega}),\ \Delta u + \kappa^2 u = 0 \text{ in } \Omega\}. \tag{15}$$

Similarly we introduce $\mathcal{C}_\kappa^-(\Omega) := \{\gamma_c(u),\ u \in \mathrm{H}^1_{\mathrm{loc}}(\Delta, \mathbb{R}^d \setminus \Omega),\ \Delta u + \kappa^2 u = 0 \text{ in } \mathbb{R}^d \setminus \overline{\Omega}\}$. These are closed subspaces of $\mathcal{H}(\Gamma)$. A first characterisation of these spaces is obtained through polarity identity. The following result is proved in [4, Lemma.6.2].

Lemma 3.1.
Take any $\mathfrak{u} \in \mathcal{H}(\Gamma)$ and $\sigma = \pm$. We have $\mathfrak{u} \in \mathcal{C}_\kappa^\sigma(\Omega) \iff [\mathfrak{u}, \mathfrak{v}]_\Gamma = 0\ \forall \mathfrak{v} \in \mathcal{C}_\kappa^\sigma(\Omega)$.



4 Calderón projectors

Alternatively, the spaces $\mathcal{C}_\kappa^\pm(\Omega)$ can be characterised by means of so-called Calderón projectors. The following result can be found e.g. in [14, Prop.3.6.2].

Proposition 4.1.
The operator $\gamma^\Omega \cdot \mathrm{G}_\kappa^\Omega$ is a continuous projector from $\mathcal{H}(\Gamma)$ into $\mathcal{H}(\Gamma)$. Its range is $\mathcal{C}_\kappa^+(\Omega)$ and its kernel is $\mathcal{C}_\kappa^-(\Omega)$. In particular $\mathcal{H}(\Gamma) = \mathcal{C}_\kappa^+(\Omega) \oplus \mathcal{C}_\kappa^-(\Omega)$.

It is customary to introduce the operator $\mathrm{A}_\kappa^\Omega := 2\{\gamma^\Omega\}\cdot \mathrm{G}_\kappa^\Omega$ which is equivalent to decomposing the Calderón projector in the following way

$$\gamma^\Omega \cdot \mathrm{G}_\kappa^\Omega = \frac{1}{2}(\mathrm{Id} + \mathrm{A}_\kappa^\Omega) \tag{16}$$

In the present section we will discuss in thorough details the structure of the operator A_κ^Ω. This operator satisfies several interesting and useful properties. First of all $\gamma^\Omega \cdot \mathrm{G}_\kappa^\Omega$ being a projector is equivalent to the identity $(\mathrm{A}_\kappa^\Omega)^2 = \mathrm{Id}$.

In the present contribution, we are interested in domain decomposition with geometric configurations involving multiple subdomains, so we pay a particular attention to the case where the boundary $\Gamma = \partial\Omega$ is multiply connected. Since, by assumption (1), we discard triple junctions, $\mathbb{R}^d \setminus \overline{\Omega}$ can be decomposed into disjoint connected components each of which induces a connected component of $\Gamma = \partial\Omega$,

$$\begin{aligned}
&\mathbb{R}^d \setminus \overline{\Omega} = \cup_{p=1}^{m_\Omega} \omega_p^c, \quad \omega_p^c \cap \omega_q^c = \emptyset \quad \text{for} \quad p \neq q,\\
&\omega_p := \mathbb{R}^d \setminus \overline{\omega}_p^c \quad \text{so that} \quad \Omega = \cap_{p=1}^{m_\Omega} \omega_p,\\
&\Gamma = \cup_{p=1}^{m_\Omega} \partial\omega_p = \cup_{p=1}^{m_\Omega} \partial\omega_p^c.
\end{aligned} \tag{17}$$

Introduce the restriction operator $\mathrm{R}_\Gamma^p : \mathcal{H}(\Gamma) \to \mathcal{H}(\partial\omega_p)$ defined by $\mathrm{R}_\Gamma^p(\mathfrak{u}) := \mathfrak{u}|_{\partial\omega_p}$. Consider also its adjoint $(\mathrm{R}_\Gamma^p)^* : \mathcal{H}(\partial\omega_p) \to \mathcal{H}(\Gamma)$ with respect to the duality pairing (10) defined by $[(\mathrm{R}_\Gamma^p)^*(\mathfrak{u}), \mathfrak{v}]_\Gamma := [\mathfrak{u}, \mathrm{R}_\Gamma^p(\mathfrak{v})]_{\partial\omega_p}$ for all $\mathfrak{u} \in \mathcal{H}(\partial\omega_p), \mathfrak{v} \in \mathcal{H}(\Gamma)$. In more explicit terms we have $(\mathrm{R}_\Gamma^p)^*(\mathfrak{u}) = \mathfrak{u}\cdot 1_{\partial\omega_p}$ (i.e. the pair $\mathfrak{u}$ extended by 0 to all of Γ). Observe that $\mathrm{Id} = \sum_{p=1}^{m_\Omega} (\mathrm{R}_\Gamma^p)^* \mathrm{R}_\Gamma^p$

in $\mathcal{H}(\Gamma)$, each $(\mathrm{R}_\Gamma^p)^*\mathrm{R}_\Gamma^p$ being a projector, and $\mathrm{Id} = \mathrm{R}_\Gamma^p \cdot (\mathrm{R}_\Gamma^p)^*$ in $\mathcal{H}(\partial\omega_p)$. As a consequence from (16) we deduce

$$\begin{aligned} &\mathrm{R}_\Gamma^p \cdot \gamma^\Omega = \gamma^{\omega_p} \quad \text{and} \quad \mathrm{G}_\kappa^\Omega \cdot (\mathrm{R}_\Gamma^p)^* = \mathrm{G}_\kappa^{\omega_p} \\ &\Longrightarrow \quad \mathrm{R}_\Gamma^p \mathrm{A}_\kappa^\Omega (\mathrm{R}_\Gamma^p)^* = \mathrm{A}_\kappa^{\omega_p} \end{aligned} \tag{18}$$

This shows that the diagonal contributions of A_κ^Ω take the form $\mathrm{A}_\kappa^{\omega_p}, p = 1 \dots m_\Omega$. Next we introduce the diagonal part $\mathrm{D}_\kappa^\Omega : \mathcal{H}(\Gamma) \to \mathcal{H}(\Gamma)$ of the operator A_κ^Ω, defined through restriction operators by

$$\mathrm{D}_\kappa^\Omega = \sum_{p=1}^{m_\Omega} (\mathrm{R}_\Gamma^p)^* \mathrm{A}_\kappa^{\omega_p} \mathrm{R}_\Gamma^p \tag{19}$$

Obviously we have $\mathrm{R}_\Gamma^p \cdot (\mathrm{R}_\Gamma^q)^* = 0$ for $p \neq q$, and since $\mathrm{Id} = \mathrm{R}_\Gamma^p \cdot (\mathrm{R}_\Gamma^p)^*$ and $(\mathrm{A}_\kappa^{\omega_p})^2 = \mathrm{Id}$. We conclude that $(\mathrm{D}_\kappa^\Omega)^2 = \mathrm{Id}$. This result was already established in [2, Lemma 6.2]. This is summarised, together with [2, Lemma 6.3], in the next proposition.

Proposition 4.2.
Decompose the operator A_κ^Ω given by (16) into its diagonal part D_κ^Ω defined by (19), and its extra-diagonal part $\mathrm{T}_\kappa^\Omega := \mathrm{A}_\kappa^\Omega - \mathrm{D}_\kappa^\Omega$. Then we have

$$(\mathrm{D}_\kappa^\Omega)^2 = \mathrm{Id} \quad \textit{and} \quad (\mathrm{T}_\kappa^\Omega)^2 = 0.$$

Since on the other hand we know that $(\mathrm{A}_\kappa^\Omega)^2 = \mathrm{Id}$, we conclude from the previous result $\mathrm{T}_\kappa^\Omega \mathrm{D}_\kappa^\Omega + \mathrm{D}_\kappa^\Omega \mathrm{T}_\kappa^\Omega = 0$. The next proposition establishes a slightly more precise result.

Proposition 4.3.
With the same notations as in the previous proposition, we have

$$\mathrm{T}_\kappa^\Omega \mathrm{D}_\kappa^\Omega = -\mathrm{T}_\kappa^\Omega \quad \textit{and} \quad \mathrm{D}_\kappa^\Omega \mathrm{T}_\kappa^\Omega = +\mathrm{T}_\kappa^\Omega.$$

Proof:

Since we already know that $\mathrm{T}_\kappa^\Omega \mathrm{D}_\kappa^\Omega + \mathrm{D}_\kappa^\Omega \mathrm{T}_\kappa^\Omega = 0$, it suffices to establish $\mathrm{D}_\kappa^\Omega \mathrm{T}_\kappa^\Omega = -\mathrm{T}_\kappa^\Omega$. According to the definition (19) we have $\mathrm{R}_\Gamma^p \mathrm{D}_\kappa^\Omega \mathrm{T}_\kappa^\Omega (\mathrm{R}_\Gamma^q)^* = \mathrm{A}_\kappa^{\omega_p} \mathrm{R}_\Gamma^p \mathrm{T}_\kappa^\Omega (\mathrm{R}_\Gamma^q)^*$. Moreover a careful inspection of the definition of A_κ^Ω yields

$$\mathrm{R}_\Gamma^p \mathrm{T}_\kappa^\Omega (\mathrm{R}_\Gamma^q)^* = \mathrm{R}_\Gamma^p (\mathrm{A}_\kappa^\Omega - \mathrm{D}_\kappa^\Omega)(\mathrm{R}_\Gamma^q)^* = \gamma^{\omega_p} \mathrm{G}_\kappa^{\omega_q}. \tag{20}$$

Take an arbitrary $\mathfrak{u} \in \mathcal{H}(\partial\omega_q)$ and denote for a moment $\psi(\boldsymbol{x}) := \mathrm{G}_\kappa^{\omega_q}(\mathfrak{u})(\boldsymbol{x})$. Since $\Gamma^q \cap \Gamma^p = \emptyset$, the function $\psi(\boldsymbol{x})$ does not admit any discontinuity through Γ^p, so that we have $\gamma^{\omega_p} \mathrm{G}_\kappa^{\omega_q}(\mathfrak{u}) = \gamma^{\omega_p}(\psi) = \gamma_c^{\omega_p}(\psi)$. In addition $\psi(\boldsymbol{x})$ is solution to the homogeneous Helmholtz equation with wave number κ (and with appropriate radiation condition) in $\mathbb{R}^d \setminus \overline{\omega}_p$ so, according to Proposition 3.1, we have $\gamma^{\omega_p} \mathrm{G}_\kappa^{\omega_p}(\gamma_c^{\omega_p}(\psi)) = 0$ and $\gamma_c^{\omega_p} \mathrm{G}_\kappa^{\omega_p}(\gamma_c^{\omega_p}(\psi)) = -\gamma_c^{\omega_p}(\psi)$. From this we obtain

$$\begin{aligned} \mathrm{A}_\kappa^{\omega_p} \mathrm{R}_\Gamma^p \mathrm{T}_\kappa^\Omega (\mathrm{R}_\Gamma^q)^* &= 2\{\gamma^{\omega_p}\} \mathrm{G}_\kappa^{\omega_p} \cdot \gamma_c^{\omega_p} \mathrm{G}_\kappa^{\omega_q} \\ &= \gamma_c^{\omega_p} \mathrm{G}_\kappa^{\omega_p} \cdot \gamma_c^{\omega_p} \mathrm{G}_\kappa^{\omega_q} = -\gamma_c^{\omega_p} \mathrm{G}_\kappa^{\omega_q}. \end{aligned}$$

This leads to the conclusion by means of the identity $\mathrm{Id} = \sum_{p=1}^{m_\Omega} (\mathrm{R}_\Gamma^p)^* \mathrm{R}_\Gamma^p$. □

5 Local Multi-Trace Formulation

Now we briefly recall the derivation of the so-called local Multi-Trace formulation (local-MTF) for the boundary value problem (2). We first need to introduce notations related to the multi-domain setting we are interested in. We will adopt more concise notations, setting $\gamma^j := \gamma^{\Omega_j}$, $\gamma_{\rm D}^j = \gamma_{\rm D}^{\Omega_j}$ and $\gamma_{\rm N}^j = \gamma_{\rm N}^{\Omega_j}$. Next we introduce a multi-trace space

$$\begin{aligned} &\mathbb{H}(\Sigma) := \mathcal{H}(\Gamma_0) \times \cdots \times \mathcal{H}(\Gamma_n) \quad \text{with} \\ &\|\mathfrak{u}\|^2_{\mathbb{H}(\Sigma)} := \|\mathfrak{u}_0\|^2_{\mathcal{H}(\Gamma_0)} + \cdots + \|\mathfrak{u}_n\|^2_{\mathcal{H}(\Gamma_n)} \\ &[\![\mathfrak{u},\mathfrak{v}]\!] := \textstyle\sum_{j=0}^n [\mathfrak{u}_j,\mathfrak{v}_j]_{\Gamma_j} \end{aligned} \tag{21}$$

for $\mathfrak{u} = (\mathfrak{u}_j)_{j=0}^n, \mathfrak{v} = (\mathfrak{v}_j)_{j=0}^n, \mathfrak{u}_j, \mathfrak{v}_j \in \mathcal{H}(\Gamma_j)$. As easily checked, the bilinear form $[\![\cdot,\cdot]\!] : \mathbb{H}(\Sigma) \times \mathbb{H}(\Sigma) \to \mathbb{C}$ puts $\mathbb{H}(\Sigma)$ in self-duality. Next we also introduce an operator $\Pi : \mathbb{H}(\Sigma) \to \mathbb{H}(\Sigma)$ whose action consists in swapping traces from both sides of each interface. For $\mathfrak{u} = (\mathfrak{u}_j), \mathfrak{v} = (\mathfrak{v}_j) \in \mathbb{H}(\Sigma)$, it is defined by

$$\begin{aligned} \Pi(\mathfrak{u}) = \mathfrak{v} \quad \Longleftrightarrow \quad & \mathfrak{u}_j = \mathrm{Q} \cdot \mathfrak{v}_k \ \text{ on } \ \Gamma_j \cap \Gamma_k, \\ & \forall j,k = 0 \ldots n, j \neq k, \quad \text{where} \quad \mathrm{Q} := \begin{bmatrix} 1 & 0 \\ 0 & -1 \end{bmatrix} \end{aligned} \tag{22}$$

Let us emphasize that, here, we assume that there is no junction point according to Assumption (1). Under this assumption the operator $\Pi : \mathbb{H}(\Sigma) \to \mathbb{H}(\Sigma)$ is continuous, but would not be continuous otherwise. This operator allows a convenient reformulation of transmission conditions i.e. if $\mathfrak{u} = (\tau_{\mu_j} \cdot \gamma^j(u))_{j=0}^n \in \mathbb{H}(\Sigma)$ where $\tau_\alpha(v,q) := (v, q/\alpha)$ and $u \in \mathrm{L}^2_{\rm loc}(\mathbb{R}^d)$ refers to the unique solution to the BVP (4)-(5), then (5) rewrites $\Pi(\mathfrak{u}) = \mathfrak{u}$. We also define $\mathrm{A}_{(\kappa)} : \mathbb{H}(\Sigma) \to \mathbb{H}(\Sigma)$ by the identity

$$\begin{aligned} &[\![\mathrm{A}_{(\kappa)}\mathfrak{u},\mathfrak{v}]\!] := \sum_{j=0}^n [\mathrm{A}^j_{\kappa_j}(\mathfrak{u}_j),\mathfrak{v}_j]_{\Gamma_j}, \\ &\text{where} \quad \mathrm{A}^j_{\kappa_j} := 2\{\gamma^j\} \cdot \mathrm{G}^{\Omega_j}_{\kappa_j} \end{aligned} \tag{23}$$

According to Proposition 4.1, each operator $(\mathrm{Id} + \mathrm{A}^j_{\kappa_j})/2 = (\{\gamma^j\} + [\gamma^j]/2) \cdot \mathrm{G}^{\Omega_j}_{\kappa_j} = \gamma^j \cdot \mathrm{G}^{\Omega_j}_{\kappa_j}$ is a projector, so that $(\mathrm{Id} + \mathrm{A}_{(\kappa)})/2$ is itself a projector mapping $\mathbb{H}(\Sigma)$ to $\mathbb{H}(\Sigma)$. The tuples $\mathfrak{u} = (\mathfrak{u}_j) \in \mathbb{H}(\Sigma)$ such that $\mathfrak{u} = \mathrm{A}_{(\kappa)}(\mathfrak{u})$ satisfy $\mathfrak{u}_j = \gamma^j \cdot \mathrm{G}^j_{\kappa_j}(\mathfrak{u}_j)$ so that $\mathfrak{u}_j \in \mathcal{C}^+_{\kappa_j}(\Omega_j)$ for all $j = 0 \ldots n$ according to Proposition 4.1.

Let us denote $\mathfrak{u}_{\rm inc} = (\gamma^0(u_{\rm inc}), 0 \ldots, 0)$, and observe that $\gamma^0(u_{\rm inc}) = \gamma^0_c(u_{\rm inc})$ since $u_{\rm inc} \in \mathscr{C}^\infty(\mathbb{R}^d)$ by elliptic regularity. As a consequence $\gamma^0(u_{\rm inc}) \in \mathcal{C}^-_{\kappa_0}(\Omega_0)$ so that $(\mathrm{Id}+\mathrm{A}^0_{\kappa_0})\gamma^0(u_{\rm inc}) = 0$ according to Proposition 4.1, and finally $(\mathrm{A}_{(\kappa)} - \mathrm{Id})\mathfrak{u}_{\rm inc} = -2\mathfrak{u}_{\rm inc}$.

Now let us recall the derivation of local-MTF for Problem (4)-(5). Let $u \in \mathrm{H}^1_{\rm loc}(\mathbb{R}^d)$ refer to the unique solution to this boundary value problem, and take $\mathfrak{u} = (\tau_{\mu_j} \cdot \gamma^j(u))_{j=0}^n \in \mathbb{H}(\Sigma)$ as the unknown of our local-MTF formulation, where $\tau_\alpha(v,q) := (v, q/\alpha)$. Equation (5) then simply rewrites $\mathfrak{u} = \Pi(\mathfrak{u})$. For $\mu = (\mu_0, \cdots, \mu_n)$ and $\mathfrak{v} = (\mathfrak{v}_j) \in \mathbb{H}(\Sigma)$, denote $\tau_{(\mu)}(\mathfrak{v}) := (\tau_{\mu_j}(\mathfrak{v}_j))_{j=0}^n$. We have in particular $\tau^{-1}_{(\mu)}(\mathfrak{u}) = (\gamma^j(u))_{j=0}^n$, so that Equation (4) can be reformulated as

$$(\mathrm{A}_{(\kappa)} - \mathrm{Id})(\tau^{-1}_{(\mu)}(\mathfrak{u}) - \mathfrak{u}_{\rm inc}) = 0.$$

Multiply this equation on the left by $\tau_{(\mu)}$, take account of the equation $\mathfrak{u} - \Pi(\mathfrak{u}) = 0$ as well as the simplifications on $\mathfrak{u}_{\rm inc}$ mentioned in the previous paragraph. Choosing an arbitrary parameter $\alpha \in \mathbb{C}$, and setting $\mathrm{A}_{(\kappa,\mu)} := \tau_{(\mu)} \cdot \mathrm{A}_{(\kappa)} \cdot \tau_{(\mu)}^{-1}$, we can combine the previously discussed identities to obtain

$$\begin{cases} \mathfrak{u} \in \mathbb{H}(\Sigma) \quad \text{such that} \\ (\mathrm{A}_{(\kappa,\mu)} - \mathrm{Id} + (1-\alpha)(\mathrm{Id} - \Pi))\mathfrak{u} = -2\tau_{(\mu)}(\mathfrak{u}_{\rm inc}) \end{cases} \tag{24}$$

Local Multi-Trace formulation (local-MTF) was initially proposed in [9] with the value $\alpha = 0$. The above formulation, that is a variant of local-MTF involving in addition the relaxation parameter α, was considered in [10]. Let us denote $\mathrm{MTF}(\alpha) : \mathbb{H}(\Sigma) \to \mathbb{H}(\Sigma)$ the operator associated to (24) defined by

$$\mathrm{MTF}_{(\kappa,\mu)}(\alpha) := \mathrm{A}_{(\kappa,\mu)} - \alpha\mathrm{Id} - (1-\alpha)\Pi \tag{25}$$

It was established in [9] that $\mathrm{MTF}_{(\kappa,\mu)}(0)$ is a continuous isomorphism for any choice of the parameters $\kappa_j, \mu_j > 0$. For the case $\mu_0 = \cdots = \mu_n = 1$, it was proved in [2] that $\mathrm{MTF}_{(\kappa,\mu)}(\alpha)$ is still an isomorphism for any choice of $\kappa_j > 0$ as soon as $\alpha \neq 1$. The value $\alpha = 1$ is clearly forbidden because in this case $\mathrm{MTF}_{(\kappa,\mu)}(1)/2$ is a non-trivial projector, hence cannot be invertible.

6 Optimal convergence result for homogenous media

Let us examine a possible iterative strategy to solve (24), denoting $\mathfrak{u}^{(k)}, k \geq 0$ the sequence of iterates constructed in this solution process. We choose here to separate diagonal and extra-diagonal terms, and apply a block-Jacobi method, considering

$$(\,\mathrm{A}_{(\kappa,\mu)} - \alpha\mathrm{Id}\,)\,\mathfrak{u}^{(k+1)} = (1-\alpha)\Pi \cdot \mathfrak{u}^{(k)} - 2\tau_{(\mu)}(\mathfrak{u}_{\rm inc}) \tag{26}$$

Here we use the identity $(\,\mathrm{A}_{(\kappa,\mu)} + \alpha\mathrm{Id}\,)(\,\mathrm{A}_{(\kappa,\mu)} - \alpha\mathrm{Id}\,) = (1-\alpha^2)\mathrm{Id}$ to compute $(\,\mathrm{A}_{(\kappa,\mu)} - \alpha\mathrm{Id}\,)^{-1}$ explicitly. On the other hand, we have $\mathrm{A}_{(\kappa,\mu)}\tau_{(\mu)}(\mathfrak{u}_{\rm inc}) = -\tau_{(\mu)}(\mathfrak{u}_{\rm inc})$, so multiplying (26) on the left with the operator $(1-\alpha^2)^{-1}(\mathrm{A}_{(\kappa,\mu)} + \alpha\mathrm{Id})$, we finally obtain the following explicit iterative scheme

$$\begin{cases} \mathfrak{u}^{(k+1)} = \mathrm{J}_\alpha(\mathfrak{u}^{(k)}) + \dfrac{2}{1+\alpha}\tau_{(\mu)}(\mathfrak{u}_{\rm inc}) \\ \text{with} \quad \mathrm{J}_\alpha := \dfrac{1}{1+\alpha}(\,\mathrm{A}_{(\kappa,\mu)} + \alpha\mathrm{Id}\,) \cdot \Pi. \end{cases} \tag{27}$$

Let us briefly discuss the convergence of this algorithm by examining the spectral radius of the iteration operator J_α. In the next result we give the explicit expression of this spectrum for a simplified case.

Proposition 6.1.
Assume that $\mu_0 = \cdots = \mu_n = 1$ and $\kappa_0 = \cdots = \kappa_n$. Then the spectrum of the operator $\mathrm{J}_\alpha : \mathbb{H}(\Sigma) \to \mathbb{H}(\Sigma)$ defined in (27) is given by $\mathfrak{S}(\mathrm{J}_\alpha) = \{+\imath\sqrt{(1-\alpha)/(1+\alpha)}, -\imath\sqrt{(1-\alpha)/(1+\alpha)}\}$.

Proof:
Let denote $\mathrm{A} = \mathrm{A}_{(\kappa,\mu)}$. Under the simplifying assumptions $\mu_0 = \cdots = \mu_n = 1$ and $\kappa_0 = \cdots = \kappa_n$, we know from [2, Thm.6.1] that $\mathrm{A} + \beta\mathrm{Id} + \gamma\Pi$ is invertible if and only if

$\beta^2 - \gamma^2 \neq 1$. From this, and $\Pi^2 = \mathrm{Id}$, we conclude that

$$\begin{aligned}
\lambda \notin \mathfrak{S}(\mathrm{A}\Pi + \alpha\Pi) &\iff (\mathrm{A} + \alpha\mathrm{Id})\Pi - \lambda\mathrm{Id} \text{ is invertible} \\
&\iff \mathrm{A} + \alpha\mathrm{Id} - \lambda\Pi \text{ is invertible} \\
&\iff \alpha^2 - \lambda^2 \neq 1 \\
&\iff \lambda \neq \pm\imath\sqrt{1-\alpha^2}.
\end{aligned}$$

□

The spectral radius $\varrho(\mathrm{J}_\alpha) := \sup\{|\lambda|,\ \lambda \in \mathfrak{S}(\mathrm{J}_\alpha)\}$ is a critical parameter as regards the convergence of the iterative scheme (27). The parameter α should be chosen so as to obtain the fastest possible convergence, hence minimizing the spectral radius $\varrho(\mathrm{J}_\alpha)$. Since $(1-\alpha)/(1+\alpha) = 0 \iff \alpha = 1$, the previous proposition suggests to take $\alpha = 1$ even though it was pointed out as a forbidden value at the end of Section 5. This choice leads to the following iterative scheme

$$\mathfrak{u}^{(k+1)} = \frac{1}{2}(\mathrm{A}_{(\kappa,\mu)} + \mathrm{Id}) \cdot \Pi(\mathfrak{u}^{(k)}) + \tau_{(\mu)}(\mathfrak{u}_{\mathrm{inc}}) \tag{28}$$

Under Hypothesis (1), the adjacency graph of the partitionning of the computational domain admits a tree structure. In this tree, vertices are identified with subdomains, and two vertices are connected by an edge if the associated subdomains are adjacent. Taking the distance between two vertices as the minimum number of edges in a path going from one vertex to the other, the depth of the adjacency graph is then defined as its diameter with respect to this distance. The next result relates the convergence of (28) to these notions.

Proposition 6.2.
Assume that $\mu_0 = \cdots = \mu_n = 1$ and $\kappa_0 = \cdots = \kappa_n$. Let $N > 0$ refer to the depth of the adjacency graph of the subdomain partition $\mathbb{R}^d = \cup_{j=0}^n \overline{\Omega}_j$. Then for $\alpha = 1$ we have $(\mathrm{J}_1)^{N+1} = 0$.

Proof:

As in the previous proof, denote $\mathrm{A} = \mathrm{A}_{(\kappa,\mu)}$. We only need to prove that $(\,(\mathrm{Id}+\mathrm{A})\Pi\,)^N = 0$. Let $\mathrm{D} : \mathbb{H}(\Sigma) \to \mathbb{H}(\Sigma)$ refer to the purely diagonal part of A defined, for $\mathfrak{u} = (\mathfrak{u}_j), \mathfrak{v} = (\mathfrak{v}_j) \in \mathbb{H}(\Sigma)$ by the formula

$$[\![\mathrm{D}(\mathfrak{u}), \mathfrak{v}]\!] = \sum_{j=0}^{n} [\mathrm{D}_\kappa^{\Omega_j}(\mathfrak{u}_j), \mathfrak{v}_j]_{\Gamma_j}. \tag{29}$$

Besides we set $\mathrm{T} := \mathrm{A} - \mathrm{D}$. Proposition 4.2 and 4.3 readily imply $\mathrm{T}^2 = 0$, $\mathrm{D}^2 = \mathrm{Id}$, $\mathrm{DT} = -\mathrm{T}$ and $\mathrm{TD} = \mathrm{T}$. In addition we know from [2, Lemma 6.2] that $\mathrm{D}\Pi = -\Pi\mathrm{D}$. Using these identities, let us first compute $(\,(\mathrm{Id}+\mathrm{A})\Pi\,)^2$. We obtain

$$\begin{aligned}
((\mathrm{Id}+\mathrm{A})\Pi)^2 &= (\mathrm{Id}+\mathrm{D}+\mathrm{T})\Pi(\mathrm{Id}+\mathrm{D}+\mathrm{T})\Pi \\
&= (\mathrm{T}\Pi)^2 + ((\mathrm{Id}+\mathrm{D})\Pi)^2 + (\mathrm{Id}+\mathrm{D})\Pi\mathrm{T}\Pi + \mathrm{T}\Pi(\mathrm{Id}+\mathrm{D})\Pi \\
&= (\mathrm{T}\Pi)^2 + \Pi(\mathrm{Id}-\mathrm{D})(\mathrm{Id}+\mathrm{D})\Pi + \Pi(\mathrm{Id}-\mathrm{D})\mathrm{T}\Pi + \mathrm{T}(\mathrm{Id}-\mathrm{D})\Pi^2 \\
&= (\mathrm{T}\Pi)^2 + 2\Pi\mathrm{T}\Pi
\end{aligned}$$

Now let us prove by recurrence that $((\mathrm{Id}+\mathrm{A})\Pi)^p = 2\Pi(\mathrm{T}\Pi)^{p-1} + (\mathrm{T}\Pi)^p$ for all $p \geq 2$. We already know that this is correct for $p = 2$. Suppose this holds for some p. Then we have

$$\begin{aligned}((\mathrm{Id}+\mathrm{A})\Pi)^{p+1} &= (\mathrm{Id}+\mathrm{D}+\mathrm{T})\Pi(2\Pi(\mathrm{T}\Pi)^{p-1} + (\mathrm{T}\Pi)^p) \\ &= 2(\mathrm{Id}+\mathrm{D}+\mathrm{T})\mathrm{T}\Pi(\mathrm{T}\Pi)^{p-2} + \Pi(\mathrm{Id}-\mathrm{D})\mathrm{T}\Pi(\mathrm{T}\Pi)^{p-1} + (\mathrm{T}\Pi)^{p+1} \\ &= 2(\mathrm{T}-\mathrm{T}+\mathrm{T}^2)\Pi(\mathrm{T}\Pi)^{p-2} + 2\Pi\mathrm{T}\Pi(\mathrm{T}\Pi)^{p-1} + (\mathrm{T}\Pi)^{p+1} \\ &= 2\Pi(\mathrm{T}\Pi)^p + (\mathrm{T}\Pi)^{p+1}\end{aligned}$$

This proves the recurrence. According to [2, Prop.6.1], we have $(\mathrm{T}\Pi)^N = 0$. From this we deduce $(\mathrm{J}_1)^{N+1} = 0$. □

Whereas $\alpha = 1$ was pointed as a forbidden value at the end of Section 5, Proposition 6.1 and 6.2 suggests that this is the value that should be considered for the iterative scheme (26). These two messages seem to be contradictory. Here is an explanation for this apparent paradox. Consider the multi-trace formulation (24) for $\alpha = -1$ which consists in finding $\mathfrak{u} \in \mathbb{H}(\Sigma)$ such that

$$(\Pi - (\mathrm{A}_{(\kappa,\mu)} + \mathrm{Id})/2)\mathfrak{u} = \tau_{(\mu)}(\mathfrak{u}_{\mathrm{inc}}). \tag{30}$$

The operator $-\mathrm{MTF}(-1)/2$ associated to this formulation is an isomorphism. Besides we know that the solution to this problem satisfies the transmission conditions $\mathfrak{u} = \Pi(\mathfrak{u})$, so we may also replace $\mathfrak{u}$ by $\Pi(\mathfrak{u})$ in (30), which leads to the equation $(\mathrm{Id}-(\mathrm{A}_{(\kappa,\mu)}+\mathrm{Id})\Pi/2)\mathfrak{u} = \tau_{(\mu)}(\mathfrak{u}_{\mathrm{inc}})$, which takes the form $(\mathrm{Id} - \mathrm{J}_\alpha)\mathfrak{u} = \tau_{(\mu)}(\mathfrak{u}_{\mathrm{inc}})$ with $\alpha = 1$. Hence, we will study the following the resolution of (30), obtained from the local-MTF formulation (24) with $\alpha = -1$, and preconditioned by Π.

7 Equivalence with Optimised Schwarz Methods

In the present section we show that, in certain situations, the iterative strategy (28) can be identified with the Optimised Schwarz Method (OSM), a well established Domain Decomposition strategy that, in its most classical form, is formulated in terms of volume PDEs. For an overview on OSM, we refer the reader to [8], and for a detailed study of OSM in the context ow wave propagation see [5, 6, 1]. We will prove that (28), can be re-written as an instance of OSM involving *exact* Dirichlet-to-Neumann maps as impedance operators. This has already been established in [3] for the simpler case where the geometric partitionning only involves two subdomains and one interface for a one dimensional problem. Our goal is to generalise this result to the present context. For the sake of simplicity, we will assume in this section that

$$\mu_0 = \mu_1 = \cdots = \mu_n. \tag{31}$$

7.1 A few observations on Dirichlet-to-Neumann (DtN) maps

In the context of domain decomposition (DDM) a more classical manner to describe solution to homogeneous PDEs relies on Dirichlet-to-Neumann (DtN) maps, also known as Steklov-Poincaré operators. There is a close connection between these maps and Calderón's projectors, and we discuss this connection here.

In this subsection, Ω will refer to any Lipschitz domain that is either bounded or the complementary of a bounded domain, and Γ will refer to its boundary. Define the continuous operator $\mathrm{DtN}_\Omega^\kappa : \mathrm{H}^{1/2}(\Gamma) \to \mathrm{H}^{-1/2}(\Gamma)$ by $\mathrm{DtN}_\Omega^\kappa(v) := \gamma_{\mathrm{N}}^\Gamma(\Phi_\Omega(v))$ where

$$\begin{aligned} &\Phi_\Omega(v) \in \mathrm{H}^1_{\mathrm{loc}}(\Delta, \overline{\Omega}) \text{ solves} \\ &\Delta\Phi_\Omega(v) + \kappa^2\Phi_\Omega(v) = 0 \quad \text{in } \Omega \\ &\gamma_{\mathrm{D}}^\Gamma(\Phi_\Omega(v)) = v \quad \text{on } \Gamma \\ &\Phi_\Omega(v) \ \kappa\text{-outgoing radiating if } \mathbb{R}^d \setminus \Omega \text{ bounded} \end{aligned} \tag{32}$$

For more details regarding the properties of the Dirichlet-to-Neumann map, we refer the reader to [11, Chap.4]. The Dirichlet-to-Neumann maps $\mathrm{DtN}_\Omega^\kappa$ are non-local, coupling any part of Γ with any other part of it. However, when Ω is not connected, this operator satisfies a localisation property.

Lemma 7.1.
Assume that $\Omega \subset \mathbb{R}^d$ is a Lipschitz subdomain such that either Ω or Ω^c is bounded. If ω refer to any connected component of Ω, we have $\mathrm{DtN}_\Omega(u)|_{\partial\omega} = \mathrm{DtN}_\omega(u|_{\partial\omega})$ for all $u \in \mathrm{H}^{1/2}(\partial\Omega)$.

Taking account of (32), the proof of the above lemma is obvious. As a consequence of this lemma, in the following we shall commit a slight abuse of notation, regarding DtN_Ω as an operator mapping $\mathrm{H}^{1/2}(\partial\omega) \to \mathrm{H}^{-1/2}(\partial\omega)$ for any connected component ω of Ω.

7.2 DtN based impedance operators

With the above notations, we introduce bounded one-to-one operators $\mathcal{S}_\Omega^\kappa : \mathrm{H}^{1/2}(\Gamma) \to \mathcal{H}(\Gamma)$ defined by

$$\mathcal{S}_\Omega^\kappa(v) := (v, \mathrm{DtN}_\Omega^\kappa(v)). \tag{33}$$

By construction we have $\mathrm{Range}(\mathcal{S}_\Omega^\kappa) = \mathcal{C}_\kappa^+(\Omega)$. Using the polarity property of Lemma 3.1, we see that $[\mathcal{S}_\Omega^\kappa(u), \mathcal{S}_\Omega^\kappa(v)]_\Gamma = 0$ for all $u, v \in \mathrm{H}^{1/2}(\Gamma)$. This latter identity rewrites $\int_\Gamma u\mathrm{DtN}_\Omega^\kappa(v)d\sigma = \int_\Gamma v\mathrm{DtN}_\Omega^\kappa(u)d\sigma$. Next introduce the bounded operator $(\mathcal{S}_{\Omega^c}^\kappa)^* : \mathcal{H}(\partial\Omega^c) \to \mathrm{H}^{-1/2}(\Gamma)$ defined by

$$(\mathcal{S}_{\Omega^c}^\kappa)^*(u, p) = \mathrm{DtN}_{\Omega^c}^\kappa(u) + p \tag{34}$$

The map $(\mathcal{S}_{\Omega^c}^\kappa)^*$ is clearly surjective. Denoting $\mathrm{Q}(v, q) := (v, -q)$ as in (22), routine calculus shows that $\langle(\mathcal{S}_{\Omega^c}^\kappa)^*(\mathfrak{u}), v\rangle_\Gamma = [\mathrm{Q}(\mathfrak{u}), \mathcal{S}_{\Omega^c}^\kappa(v)]_\Gamma$ for all $\mathfrak{u} \in \mathcal{H}(\Gamma)$ and all $v \in \mathrm{H}^{1/2}(\Gamma)$. From this formula, and the polarity property of Lemma 3.1, we deduce that $\mathrm{Ker}((\mathcal{S}_{\Omega^c}^\kappa)^*) = \mathrm{Q}\cdot\mathcal{C}_\kappa^+(\Omega^c) = \mathcal{C}_\kappa^-(\Omega)$. Finally let us consider the operator

$$(\mathcal{S}_{\Omega^c}^\kappa)^*\mathcal{S}_\Omega^\kappa = \mathrm{DtN}_{\Omega^c}^\kappa + \mathrm{DtN}_\Omega^\kappa \tag{35}$$

Since $\mathcal{H}(\Gamma) = \mathcal{C}_\kappa^-(\Omega) \oplus \mathcal{C}_\kappa^+(\Omega)$ and, on the other hand, $\mathcal{S}_\Omega^\kappa$ maps onto $\mathcal{C}_\kappa^+(\Omega)$, and $\mathcal{C}_\kappa^-(\Omega)$ is exactly the kernel of $(\mathcal{S}_{\Omega^c}^\kappa)^*$, we conclude that $(\mathcal{S}_{\Omega^c}^\kappa)^*\mathcal{S}_\Omega^\kappa : \mathrm{H}^{+1/2}(\Gamma) \to \mathrm{H}^{-1/2}(\Gamma)$ is a bijection. Finally we claim that

$$\gamma^\Omega \cdot \mathrm{G}_\kappa^\Omega = \mathcal{S}_\Omega^\kappa((\mathcal{S}_{\Omega^c}^\kappa)^*\mathcal{S}_\Omega^\kappa)^{-1}(\mathcal{S}_{\Omega^c}^\kappa)^*. \tag{36}$$

Indeed the right hand side above is clearly a projector whose kernel is $\mathcal{C}_\kappa^-(\Omega)$ and range is $\mathcal{C}_\kappa^+(\Omega)$, and these properties characterise $\gamma^\Omega \cdot \mathrm{G}_\kappa^\Omega$. This factorised form leads in particular to the identity

$$(\mathcal{S}_{\Omega^c}^\kappa)^*\gamma^\Omega \cdot \mathrm{G}_\kappa^\Omega = (\mathcal{S}_{\Omega^c}^\kappa)^*. \tag{37}$$

7.3 Reformulation of the multi-trace iterative algorithm

We now come back to the geometrical setting of Section 1. First of all let us denote $\mathfrak{u}^\infty = (\mathfrak{u}_j^\infty)_{j=0}^n \in \mathbb{H}(\Sigma)$ the unique solution to (24), so that (28) rewrites $\mathfrak{u}^{(k+1)} - \mathfrak{u}^\infty = (1/2)(\mathrm{Id} + \mathrm{A}_{(\kappa)})\Pi(\mathfrak{u}^{(k)} - \mathfrak{u}^\infty)$ under the assumption (31) that $\mu_0 = \cdots = \mu_n$. According to Proposition 4.1 we have $\mathrm{Range}(\mathrm{Id} + \mathrm{A}_{(\kappa)}) = \Pi_{j=0}^n \mathcal{C}^+_{\kappa_j}(\Omega_j)$, so that $\mathfrak{u}_j^{(k)} - \mathfrak{u}_j^\infty \in \mathcal{C}^+_{\kappa_j}(\Omega_j)$ for $k \geq 1$. As a consequence, denoting

$$\psi_j^k(\boldsymbol{x}) := \mathrm{G}_{\kappa_j}^{\Omega_j}(\mathfrak{u}_j^{(k)} - \mathfrak{u}_j^\infty)(\boldsymbol{x}), \boldsymbol{x} \in \Omega_j$$

we have $\gamma^j(\psi_j^k) = \mathfrak{u}_j^{(k)} - \mathfrak{u}_j^\infty$ for $k \geq 1$. Multiplying (28) on the left with $\mathrm{diag}_{j=0\ldots n}((\mathrm{S}_{\Omega_j^c}^{\kappa_j})^*)$, and taking account of (37), we obtain

$$\begin{array}{l} \mathrm{S}^*_{(\kappa)}(\mathfrak{u}^{(k+1)} - \mathfrak{u}^\infty) = \mathrm{S}^*_{(\kappa)}\Pi(\mathfrak{u}^{(k)} - \mathfrak{u}^\infty) \\ \text{where} \quad \mathrm{S}^*_{(\kappa)}\mathfrak{u} := ((\mathcal{S}_{\Omega_j}^{\kappa_j})^*\mathfrak{u}_j)_{j=0}^n. \end{array} \tag{38}$$

Note that $(\mathcal{S}_{\Omega_j}^{\kappa_j})^*(\mathfrak{u}_j^{(k)} - \mathfrak{u}^\infty) = \mathrm{DtN}_{\Omega_j^c}^{\kappa_j}(\psi_j^k|_{\Gamma_j}) + \partial_{n_j}\psi_j^k|_{\Gamma_j}$ The term in the right hand side of (38) can be interpreted in a similar manner, taking account of the definition of the transmission operator Π given by (22). Besides according to Lemma 7.1 applied with $\Omega = \Omega_j^c$, the operator $\mathrm{DtN}_{\Omega_j^c}^{\kappa_j}$ maps $\mathrm{H}^{1/2}(\Gamma_{j,p}) \to \mathrm{H}^{-1/2}(\Gamma_{j,p})$ for any $p \neq j$. This finally leads to the recurrence

$$\begin{array}{l} \partial_{n_j}\psi_j^{k+1}|_{\Gamma_{j,p}} + \mathrm{DtN}_{\Omega_j^c}^{\kappa_j}(\psi_j^{k+1}|_{\Gamma_{j,p}}) \\ \qquad = -\partial_{n_p}\psi_p^k|_{\Gamma_{j,p}} + \mathrm{DtN}_{\Omega_j^c}^{\kappa_j}(\psi_p^k|_{\Gamma_{j,p}}) \quad \text{on } \Gamma_{j,p}, \\ \qquad \forall j, p = 0\ldots n,\ j \neq p \quad \forall k \geq 1. \end{array} \tag{39}$$

This recurrence defines OSM, see e.g. [5, Eq.(93)], [1, Eq.(4)] or [12, Eq.(12)], with $\mathrm{DtN}_{\Omega_j^c}^{\kappa_j}$ taken as impedance in subdomain Ω_j. Formula (39) reveals a strong analogy between Optimised Schwarz Methods and local Multi-Trace formulations solved by a block Jacobi strategy. From this perspective, let us point a strong feature shared by these two methods. The nilpotence property exhibited in Proposition 6.2 shows that, in the case of an homogeneous propagation medium, the iterative algorithm (28) converges in a number of steps related to the depth of the adjacency graph of the subdomain partition. As presented in [12, Result 3.1], when the impedance operator is chosen to be the exact exterior Dirichlet-to-Neumann map, the Optimised Schwarz Method also converges in finite number of steps related to the depth of the adjacency graph.

8 Numerical evidences

In this section, we present numerical results conducted on PDEs in 2D that confirm the conclusions of the previous sections. Denote $\mathrm{D}(\boldsymbol{x}, r)$ the disk of center $\boldsymbol{x}$ and radius $r > 0$. We introduce two geometric configurations that we will use in our numerical experiences, and that are defined as follows.

Configuration I In the first configuration, represented in Figure 1, we look at centered nested disks. Considering a sequence of radii $r_j = n - j$, we set $\Omega_0 := \mathbb{R}^2 \setminus \overline{\mathrm{D}}(0, r_0)$, and then $\Omega_j = \mathrm{D}(0, r_{j-1}) \setminus \overline{\mathrm{D}}(0, r_j)$, $j = 1\ldots n-1$ and $\Omega_n = \mathrm{D}(0, 1)$. In this configuration, the depth of the adjacency graph equals n i.e. it grows with the number of subdomains.

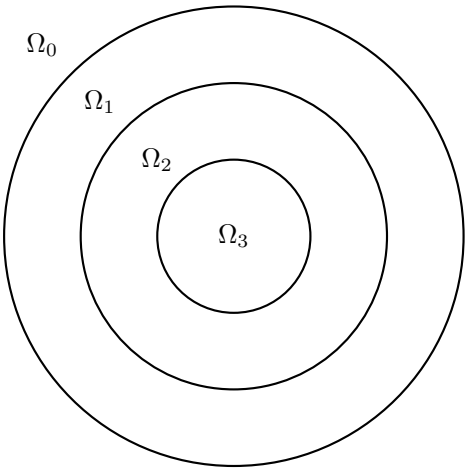


Figure 1: Configuration I

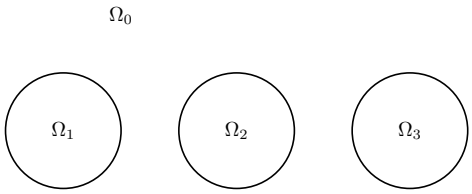


Figure 2: configuration II

Configuration II In the second configuration, represented in Figure 2, we consider a sequence of centers $\boldsymbol{x}_j = (3 \cdot (j-1), 0)$, and we consider translated unit disks $\Omega_j = \mathrm{D}(\boldsymbol{x}_j, 1), j = 1 \dots n$ as well as $\Omega_0 = \mathbb{R}^2 \setminus (\overline{\Omega}_1 \cup \cdots \cup \overline{\Omega}_n)$. In this configuration, the depth of the adjacency graph systematically equals 1, so it does not grow with n.

The point of these geometries is to have one test case where the depth of the adjacency graph increases linearly, which corresponds to the configuration I, and another test case where this depth is constant, which is configuration II. This two test cases will allow us to illustrate numerically Proposition 6.2.

8.1 Discretisation

We solve Equation (24) with a Galerkin discretisation using the BEMTool library*. We approximate $\mathbb{H}(\Sigma)$ with the space $\mathrm{V}_h = \Pi_{j=0}^{n} \mathrm{V}_h(\Gamma_j) \times \mathrm{V}_h(\Gamma_j)$, where each $\mathrm{V}_h(\Gamma_j)$ is $\mathbb{P}_1$-Lagrange function space over a regular mesh (here a set of straight panels forming a polygonal line) with h as the maximal length of the panels. After discretisation, Equation (24) becomes

$$(\mathbf{A}_{(\kappa)} - \mathbf{M} + (1-\alpha)(\mathbf{M} - \mathbf{\Pi}))\mathfrak{u}_h = -2\mathbf{M}\mathfrak{u}_{h,\mathrm{inc}}, \tag{40}$$

where $\mathfrak{u}_h$, $\mathfrak{u}_{\mathrm{inc},h} \in \mathrm{V}_h$ and $\mathbf{A}_{(\kappa)}$, $\mathbf{M}$ and $\mathbf{\Pi}$ are the Galerkin matrices associated to, respectively, $\mathrm{A}_{(\kappa)}$, Id and Π. The discrete counterpart of the multi-trace operator will be denoted $\mathbf{MTF}_{(\kappa)}(\alpha) := \mathbf{A}_{(\kappa)} - \alpha\mathbf{M} - (1-\alpha)(\mathbf{M} - \mathbf{\Pi})$. We will be interested in the following system

$$-\frac{1}{2}\mathbf{MTF}_{(\kappa)}(\alpha)\mathfrak{u}_h = \mathbf{M}\mathfrak{u}_{\mathrm{inc},h}, \tag{41}$$

for several values of α and various choices of $\kappa_0, \dots, \kappa_n$ and $\mu_0, \dots, \mu_n$. As explained at the end of Section 6, a good choice would be $\alpha = -1$, taking $\mathbf{\Pi}$ as right preconditionner, so that in the homogeneous case, $\mathbf{MTF}_{(\kappa)}(\alpha) \cdot \mathbf{\Pi}^{-1}$ approximates a nilpotent perturbation of the identity.

*`https://github.com/xclaeys/bemtool`

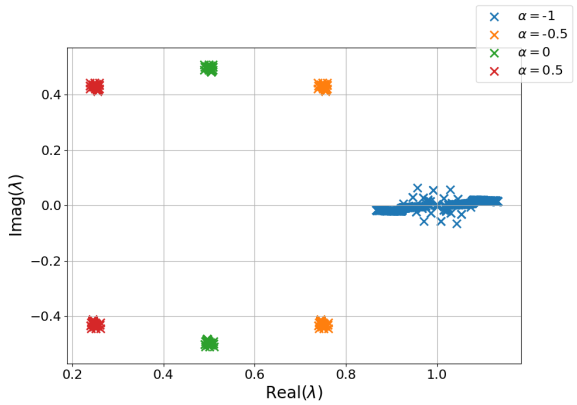


Figure 3: Spectrum of $-\mathbf{MTF}_{(\kappa)}(\alpha)/2$ with configuration I and $n = 3$

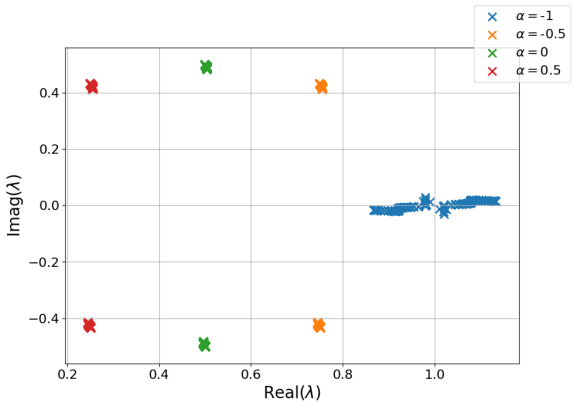


Figure 4: Spectrum of $-\mathbf{MTF}_{(\kappa)}(\alpha)/2$ with configuration II and $n = 3$

In [9, Section 5.3], the authors introduced a preconditioning strategy for (24) with $\alpha = 0$ where the diagonal part of the operator $\mathrm{MTF}_{(\kappa)}(0)$, that is to say $\mathrm{A}_{(\kappa)}$, is used as a preconditioner. However we have the following relation

$$\begin{aligned}\mathrm{A}_{(\kappa)}\mathrm{MTF}_{(\kappa)}(0) &= \mathrm{A}_{(\kappa)}(\mathrm{A}_{(\kappa)} - \Pi) = \mathrm{Id} - \mathrm{A}_{(\kappa)}\Pi \\ &= -(\mathrm{A}_{(\kappa)} - \Pi)\Pi = -\mathrm{MTF}_{(\kappa)}(0)\Pi,\end{aligned}$$

using $\mathrm{A}^2_{(\kappa)} = \mathrm{Id}$ and $\Pi^2 = \mathrm{Id}$. So that, the preconditioning strategy suggested in [9, Section 5.3] corresponds also to a right preconditioning by Π for the case $\alpha = 0$.

8.2 Spectrum

We first examine the spectrum of the local multi-trace operator for various values of α. At the continuous level, we are interested in finding $\mathfrak{u} \neq 0$ and $\lambda \in \mathbb{C}$ such that $-(1/2)\mathrm{MTF}_{(\kappa)}(\alpha)\Pi^{-1}\mathfrak{u} = \lambda\mathfrak{u}$, which is equivalent to determining $\mathfrak{v} \neq 0$ and $\lambda \in \mathbb{C}$ such that $\mathrm{MTF}_{(\kappa)}(\alpha)\mathfrak{v} = -2\lambda\Pi\mathfrak{v}$. The discrete counterpart of this eigenvalue problem writes

$$-\frac{1}{2}\mathbf{MTF}_{(\kappa)}(\alpha)\mathfrak{v}_h = \lambda\mathbf{\Pi}\mathfrak{v}_h.$$

We show the results in Figures 3 and 4 for the homogeneous case $\kappa_0 = \kappa_1 = \kappa_2 = \kappa_3 = 1$ and $\mu_0 = \mu_1 = \mu_2 = \mu_3 = 1$, we see that for $\alpha \neq -1$, there are two clusters of eigenvalues, while there is only one cluster for $\alpha = -1$ around the real value 1.

8.3 Convergence

We now solve our problem (41) using GMRes with 10000 as maximum number of iterations and a relative tolerance of 10^{-5}, for several α, $\mathbf{\Pi}$ as a preconditioner and a varying number of interfaces. Notice that in the case where $\kappa_j = 1$ for every $0 \leq j \leq n$, we know that the solution is u_{inc} so that we checked that the relative L_2 norm between the approximated solution $\mathfrak{u}_h$ and $\mathfrak{u}_{\mathrm{inc}}$ is of order of 10^{-6} with our discretisation for every test cases and independently of the number of interfaces, so that they are comparable. In this homogeneous case, we

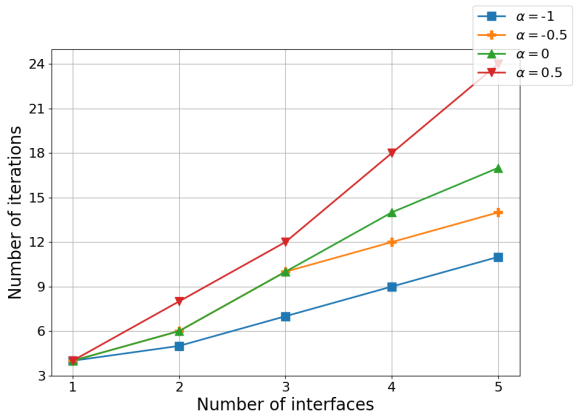


Figure 5: Number of iterations solving Equation (41) with configuration I, $\mathbf{\Pi}$ as as preconditioner and a homogeneous material

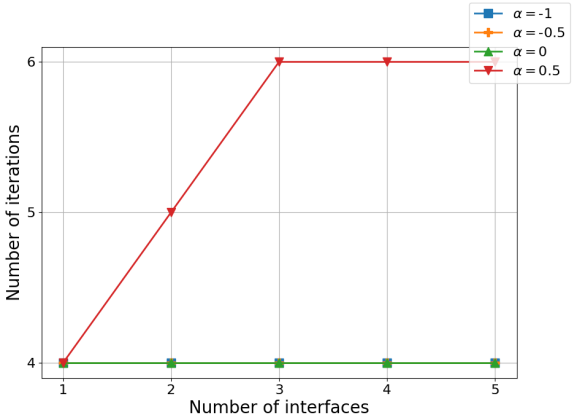


Figure 6: Number of iterations solving Equation (41) with configuration II, $\mathbf{\Pi}$ as as preconditioner and a homogeneous material

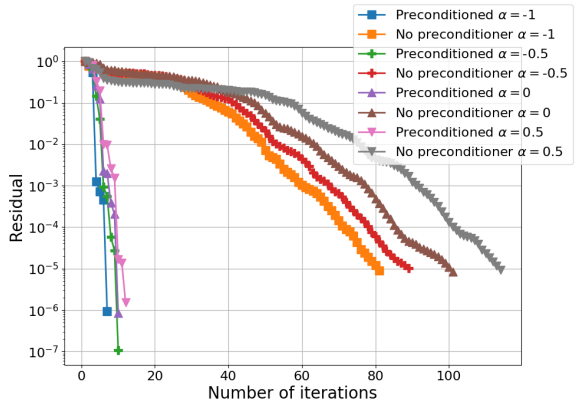


Figure 7: Residual history solving Equation (41) with configuration I and a homogeneous material

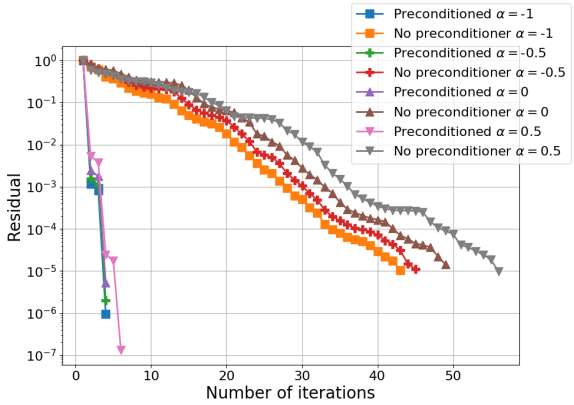


Figure 8: Residual history solving Equation (41) with configuration II and a homogeneous material

obtain Figures 5 and 6 where we see that the number of iterations increases linearly in the case of configuration I and stagnates in the case of configuration II for $\alpha = -1$, which is consistent with Proposition 6.2 and the remark at the end of Section 6, even if we do not obtain exactly that the number of iterations is equal to the number of interfaces because of numerical approximation. In Figure 5, we also remark that the closer α is to -1, the smaller is the number of iterations. This last remark will prevail in all our numerical tests.

We show in Figures 7 and 8 the residual history during the GMRes iterations for three interfaces and compare them to the case without preconditioner. We can observe the efficiency of this simple preconditioner for $\alpha = -1$, going from 81 iterations without preconditioner to 7 iterations with $\mathbf{\Pi}$ as a preconditioner in the case of the configuration I, and from 43 to 4 in the case of configuration II.

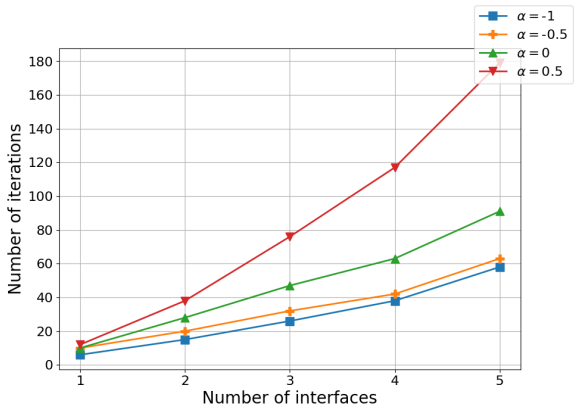


Figure 9: Number of iterations solving Equation (41) with configuration I, $\mathbf{\Pi}$ as as preconditioner and (κ) obtained randomly between 1 and 3

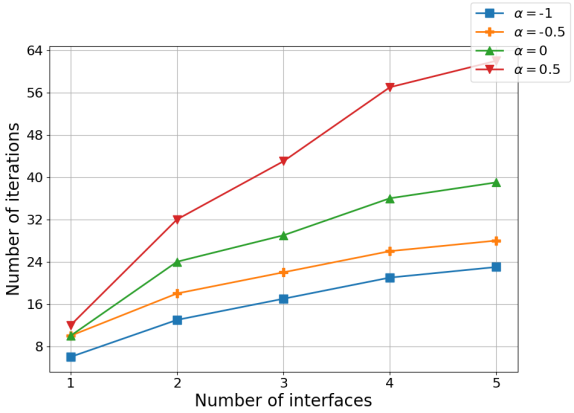


Figure 10: Number of iterations solving Equation (41) with configuration II, $\mathbf{\Pi}$ as as preconditioner and (κ) obtained randomly between 1 and 3

All the calculus in Sections 6 and 7 hold in the case of a homogeneous material, $\kappa_0 = \kappa_1 = \cdots = \kappa_n$. Differences between κ_i and κ_j with $i \neq j$ will only induce compact perturbations of the formulation. That is why, we expect the behavior observed previously to hold to some extent. We first consider the following case: $\kappa_0 = 1.00002$, $\kappa_1 = 1.26308$, $\kappa_2 = 2.51121$, $\kappa_3 = 1.9173$, $\kappa_4 = 2.06553$ and $\kappa_5 = 1.43792$, where the values between 1 and 3 were obtained randomly and we keep $\mu_0 = \mu_1 = \cdots = \mu_5 = 1$. In this case, we obtain Figures 9 and 10 where we can see that we no longer have a linear increasing or constant behavior of the number of iterations with the number of interfaces. But we see that the value $\alpha = -1$ associated with our preconditioner is still the one leading to the smallest number of iterations. For example, we can see Figures 11 and 12, where we show the residual history for $n = 3$, that for $\alpha = -1$, we obtain 126 iterations without preconditioner and 26 with $\mathbf{\Pi}$ as a preconditioner in the case of configuration I while we obtain 74 iterations without preconditioner and 17 iterations with $\mathbf{\Pi}$ as a preconditioner in the case of configuration II. Of course, if the difference between the κ_j increases, the number of iterations will increase, as we can see in Figures 13, 14, 15 and 16 where we show the results from the same kind of numerical experiences but with $\kappa_0 = 1.00039$, $\kappa_1 = 7.57689$, $\kappa_2 = 38.7803$, $\kappa_3 = 23.9325$, $\kappa_4 = 27.6384$ and $\kappa_5 = 11.948$, theses values between 1 and 40 being again obtained randomly. We observe in these figures that the number of iterations greatly increases, even if the value $\alpha = -1$ is still giving the best results. For example, for $\alpha = -1$, it does not converge without preconditioner and we obtain 587 iterations with $\mathbf{\Pi}$ as a preconditioner in the case of configuration I, while it goes from 507 iterations without a preconditioner to 86 with $\mathbf{\Pi}$ as a preconditioner in the case of configuration II. The fact that higher contrasts in (κ) make such an impactlead us to think that the formulation needs be modified in this case, even if our preconditioner helps to lower the increase of the number of iterations.

Figures 17, 18, 19 and 20 show the results for the same numerical tests as before but with $\kappa_j = 1$ if j is even and $\kappa_j = 10$ otherwise in the case of configuration I and $\kappa_0 = 1$ and $\kappa_j = 10$ with $1 \leq j \leq n$ for configuration II. The same observations as in the preceding paragraph can be made. For example, for $\alpha = -1$ and $n = 3$, it does not converge without preconditioner

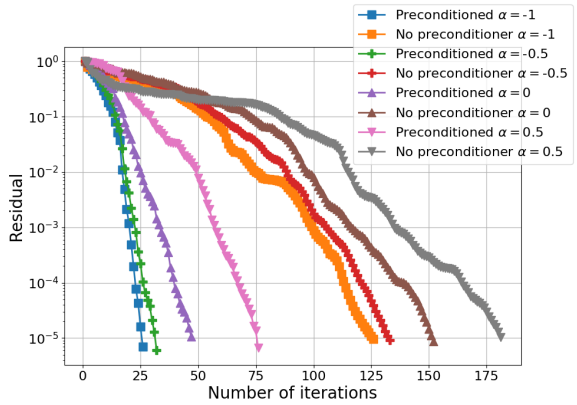


Figure 11: Residual history solving Equation (41) with configuration I and (κ) obtained randomly between 1 and 3

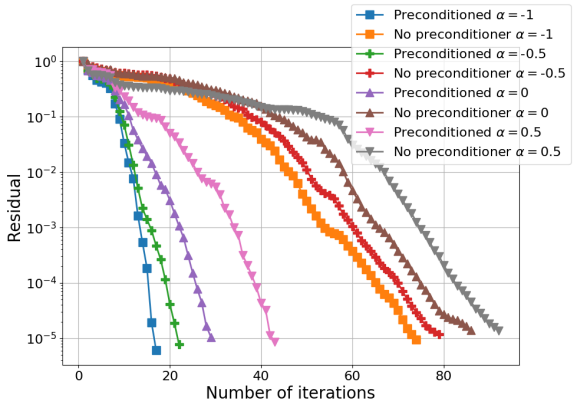


Figure 12: Residual history solving Equation (41) with configuration II and (κ) obtained randomly between 1 and 3

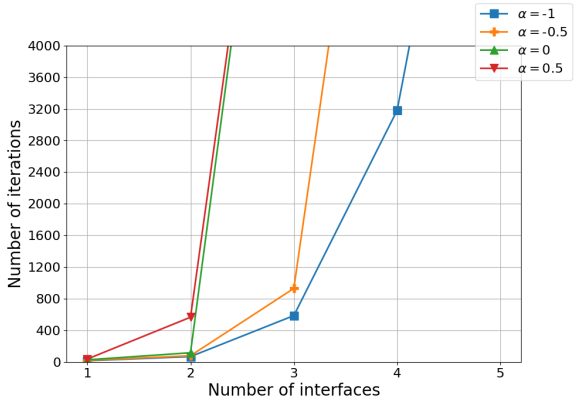


Figure 13: Number of iterations solving Equation (41) with configuration I, $\mathbf{\Pi}$ as as preconditioner and (κ) obtained randomly between 1 and 40

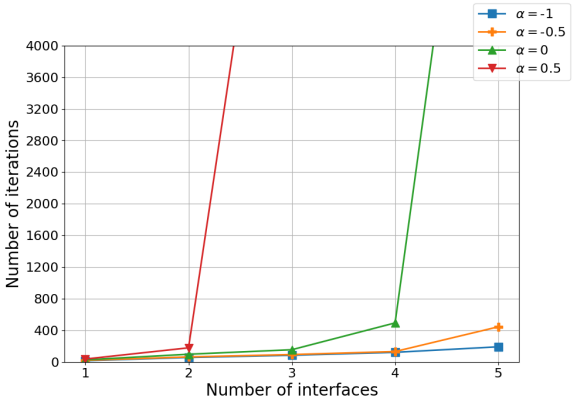


Figure 14: Number of iterations solving Equation (41) with configuration II, $\mathbf{\Pi}$ as as preconditioner and (κ) obtained randomly between 1 and 40

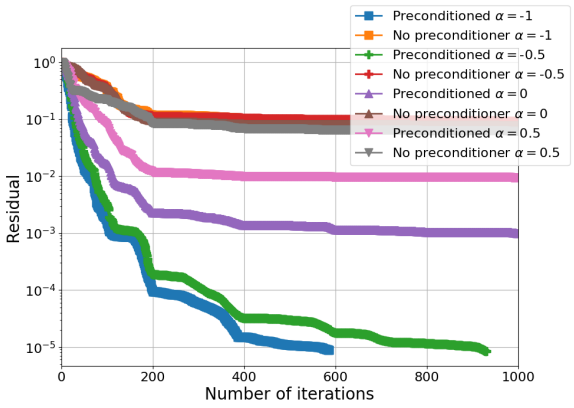


Figure 15: Residual history solving Equation (41) with configuration I and (κ) obtained randomly between 1 and 40

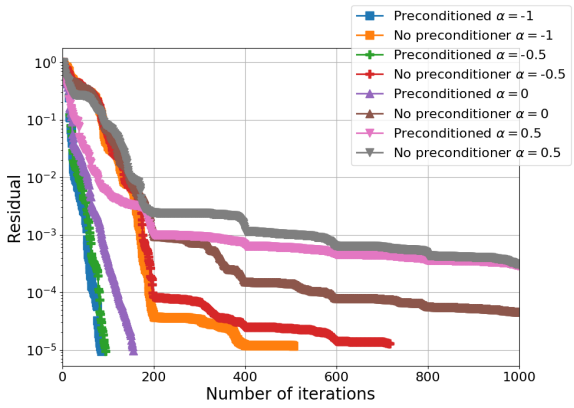


Figure 16: Residual history solving Equation (41) with configuration II and (κ) obtained randomly between 1 and 40

and we obtain 180 iterations with $\mathbf{\Pi}$ as a preconditioner in the case of the configuration I, and it goes from 149 iterations to 57 using $\mathbf{\Pi}$ as a preconditioner in the case of configuration II.

Finally, we take $\kappa_0 = \cdots = \kappa_n = 1$ and $\mu_0 = 1.00078$, $\mu_1 = 14.1538$, $\mu_2 = 76.5605$, $\mu_3 = 46.865$, $\mu_4 = 54.2767$ and $\mu_5 = 22.8959$, random values between 1 and 100, to study the influence of a perturbation coming from (μ). According to Figures 21, 22, 23 and 24, we see that the impact on the number of iterations due to this kind of perturbation is weaker that the one due to a perturbation on (κ). Indeed, in this case, we see Figures 21 and 22 that it still converges in every test cases without preconditioner, contrary to the last two numerical experiences. For examples, for $\alpha = -1$ and $n = 3$, it goes from 3187 iterations without preconditioner to 35 with our preconditioner for configuration I, while it goes from 82 to 29 using our preconditioner in configuration II.

Acknowledgement

This work received support from the ANR research grant ANR-15-CE23-0017-01.

References

[1] Y. Boubendir, X. Antoine, and C. Geuzaine. A quasi-optimal non-overlapping domain decomposition algorithm for the Helmholtz equation. *J. Comput. Phys.*, 231(2):262–280, 2012.

[2] X. Claeys. Essential spectrum of local multi-trace boundary integral operators. *IMA J. Appl. Math.*, 81(6):961–983, 2016.

[3] X. Claeys, V. Dolean, and M. J. Gander. An introduction to multi-trace formulations and associated domain decomposition solvers. *Appl. Numer. Math.*, 135:69–86, 2019.

[4] X. Claeys and R. Hiptmair. Multi-trace boundary integral formulation for acoustic scattering by composite structures. *Comm. Pure Appl. Math.*, 66(8):1163–1201, 2013.

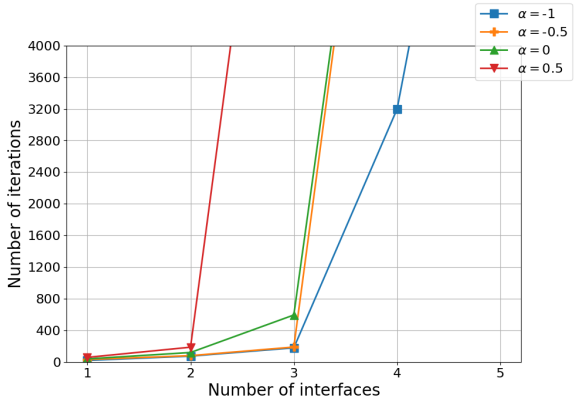


Figure 17: Number of iterations solving Equation (41) with configuration I, $\mathbf{\Pi}$ as as preconditioner, $\kappa_j = 1$ if j is even and $\kappa_j = 10$ for $0 \leq j \leq n$

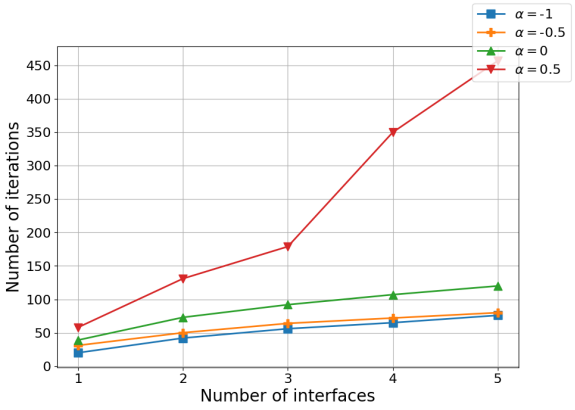


Figure 18: Number of iterations solving Equation (41) with configuration II, $\mathbf{\Pi}$ as as preconditioner, $\kappa_0 = 1$ and $\kappa_j = 10$ otherwise for $1 \leq j \leq n$

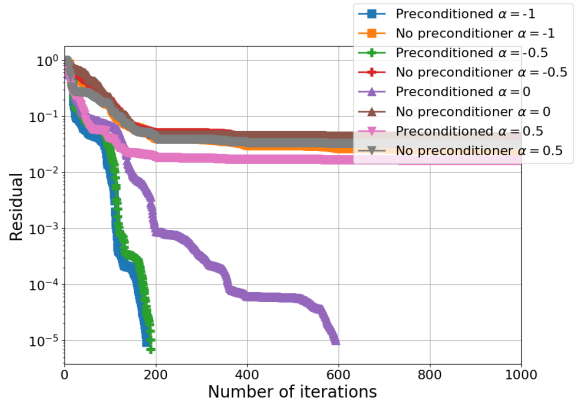


Figure 19: Residual history solving Equation (41) with configuration I, $\mathbf{\Pi}$ as as preconditioner, $\kappa_j = 1$ if j is even and $\kappa_j = 10$ for $0 \leq j \leq n$

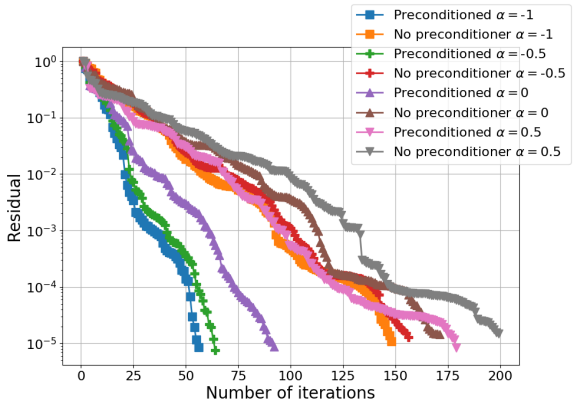


Figure 20: Residual history solving Equation (41) with configuration II, $\mathbf{\Pi}$ as as preconditioner, $\kappa_0 = 1$ and $\kappa_j = 10$ for $1 \leq j \leq n$

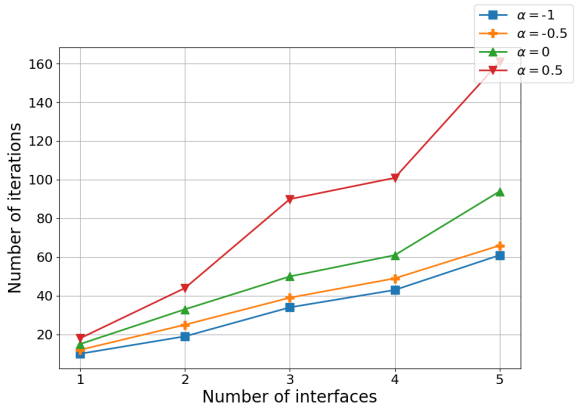


Figure 21: Number of iterations solving Equation (41) with configuration I, $\mathbf{\Pi}$ as as preconditioner, $\kappa_j = 1$ if j is even and $\kappa_j = 10$ for $0 \leq j \leq n$

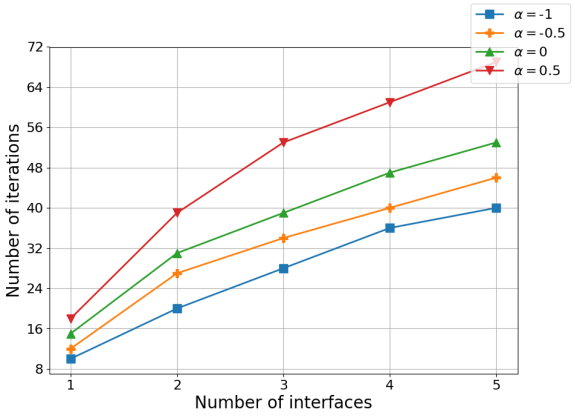


Figure 22: Number of iterations solving Equation (41) with configuration II, $\mathbf{\Pi}$ as as preconditioner, $\kappa_0 = 1$ and $\kappa_j = 10$ otherwise for $1 \leq j \leq n$

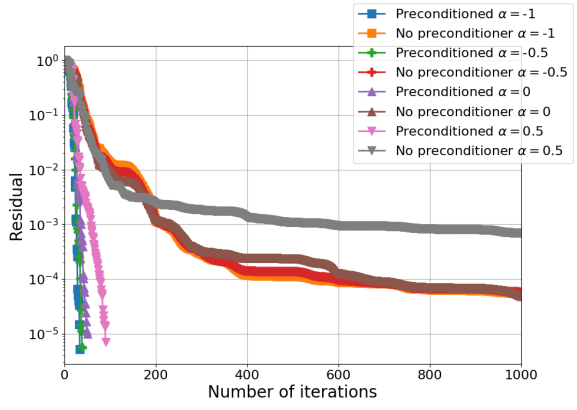


Figure 23: Residual history solving Equation (41) with configuration I, $\mathbf{\Pi}$ as as preconditioner, $\kappa_j = 1$ if j is even and $\kappa_j = 10$ for $0 \leq j \leq n$

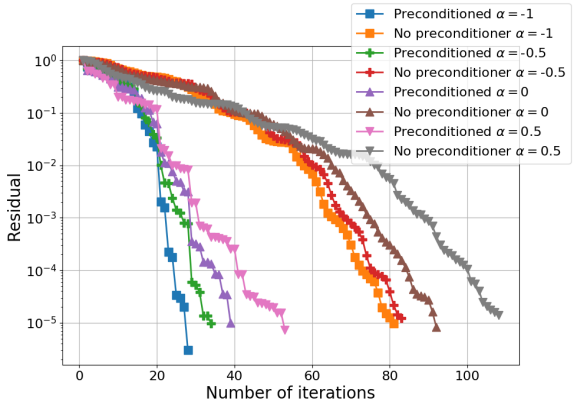


Figure 24: Residual history solving Equation (41) with configuration II, $\mathbf{\Pi}$ as as preconditioner, $\kappa_0 = 1$ and $\kappa_j = 10$ for $1 \leq j \leq n$

[5] F. Collino, S. Ghanemi, and P. Joly. Domain decomposition method for harmonic wave propagation: a general presentation. *Comput. Methods Appl. Mech. Engrg.*, 184(2-4):171–211, 2000. Vistas in domain decomposition and parallel processing in computational mechanics.

[6] Bruno Després. *Méthodes de décomposition de domaine pour les problèmes de propagation d'ondes en régime harmonique. Le théorème de Borg pour l'équation de Hill vectorielle.* Institut National de Recherche en Informatique et en Automatique (INRIA), Rocquencourt, 1991. Thèse, Université de Paris IX (Dauphine), Paris, 1991.

[7] V. Dolean and M.J. Gander. Multitrace formulations and Dirichlet-Neumann algorithms. In *Domain decomposition methods in science and engineering XXII*, volume 104 of *Lect. Notes Comput. Sci. Eng.*, pages 147–155. Springer, Cham, 2016.

[8] M.J. Gander. Optimized Schwarz methods. *SIAM J. Numer. Anal.*, 44(2):699–731, 2006.

[9] R. Hiptmair and C. Jerez-Hanckes. Multiple traces boundary integral formulation for Helmholtz transmission problems. *Adv. Comput. Math.*, 37(1):39–91, 2012.

[10] R. Hiptmair, C. Jerez-Hanckes, J.-F. Lee, and Z. Peng. Domain decomposition for boundary integral equations via local multi-trace formulations. In *Domain decomposition methods in science and engineering XXI*, volume 98 of *Lect. Notes Comput. Sci. Eng.*, pages 43–57. Springer, Cham, 2014.

[11] W. McLean. *Strongly elliptic systems and boundary integral equations.* Cambridge University Press, Cambridge, 2000.

[12] F. Nataf and F. Rogier. Factorization of the convection-diffusion operator and the Schwarz algorithm. *Math. Models Methods Appl. Sci.*, 5(1):67–93, 1995.

[13] J.-C. Nédélec. *Acoustic and electromagnetic equations*, volume 144 of *Applied Mathematical Sciences.* Springer-Verlag, New York, 2001. Integral representations for harmonic problems.

[14] S.A. Sauter and C. Schwab. *Boundary element methods*, volume 39 of *Springer Series in Computational Mathematics.* Springer-Verlag, Berlin, 2011.